

Similarity relations of the ICRF systems between two tokamaks, JET and ITER

Cite as: AIP Conference Proceedings **2254**, 070004 (2020); <https://doi.org/10.1063/5.0013589>
Published Online: 16 September 2020

Jungpyo Lee, Roberto Bilato, Hyeonjun Lee, et al.



View Online



Export Citation

ARTICLES YOU MAY BE INTERESTED IN

[Three-dimensional RF and circuit modelling of the revised ITER ICRF launcher design](#)
AIP Conference Proceedings **2254**, 070008 (2020); <https://doi.org/10.1063/5.0014200>

[Recent improvements to the ICRF antenna coupling code “RAPLICASOL”](#)
AIP Conference Proceedings **2254**, 070005 (2020); <https://doi.org/10.1063/5.0013518>

[The RF heating systems of Italian DTT](#)
AIP Conference Proceedings **2254**, 070009 (2020); <https://doi.org/10.1063/5.0014866>

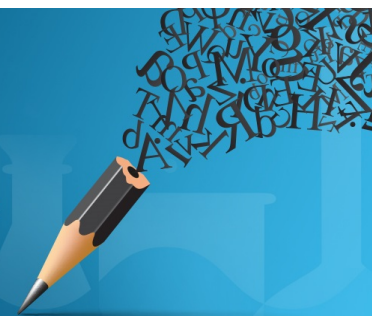


Author Services

English Language Editing

High-quality assistance from subject specialists

LEARN MORE



Similarity relations of the ICRF systems between two tokamaks, JET and ITER

Jungpyo Lee^{1,2,a)}, Roberto Bilato³, Hyeonjun Lee¹, Erwin F. Jaeger⁴

¹Hanyang University, Nuclear Engineering Department, Seoul, South Korea

²MIT Plasma Science and Fusion Center, Cambridge, MA, 02139, USA

³Max-Planck-Institute for Plasma Physics, Boltzmannstr. 2, Garching, Germany

⁴XCEL Engineering, Oak Ridge, TN, 37830, USA

a)jungpyo@hanyang.ac.kr

Abstract. We present theoretical conditions of the similarity between two equivalent RF systems in tokamaks, and find important deviations from the similarity relations. The exact similarity conditions are unlikely attainable in real experiments because of many practical and physical constraints. We found that three combinations of the scaling parameters (D_1 , D_2 , D_3) sufficiently describe three important ICRF phenomena (optimized minority fractions, power decompositions, and effective temperatures) by capturing damping mechanisms, kinetic effects, FLR effects, and Doppler effects, unless the deviations are significant. In this proceeding, we compare the Helium-3 minority heating scenarios in Hydrogen plasmas between JET and ITER

1. INTRODUCTION

It is important to know the degree of the similarity when using the dedicated experiment of a small system to predict a large system result. In this study, we present theoretical conditions of the similarity between two equivalent RF systems in tokamaks, and find important deviations from the similarity relations. The RF wave propagation and damping patterns in plasmas are exactly equivalent in two tokamaks (e.g. JET and ITER), of which one size is twice as large as the other, if the larger tokamak has a half of the magnetic field, a half of the wave frequency, a quarter of the density, the same temperature, and a half of the RF power of the smaller tokamak [1]. More generally, the scaling conditions of the exact similarity are given by

$$\eta_\omega = \eta_B, \eta_n = \eta_B^2, \eta_R = \eta_B^{-1}, \eta_P = \eta_B, \eta_{n\Phi} = \eta_{I_p} = \eta_T = 1, \quad (1)$$

where η_x is the scaling factor between two tokamaks for the wave frequency ω , the magnetic fields B , the machine size R , the plasma current I_p , the plasma density n , temperature T , the wave total power P , toroidal mode number n_Φ . These similarity relations are verified by the coupled codes, AORSA-ECOM-CQL3D, in which the Maxwell's equation, Grad-Shafranov equation, and Fokker-Planck equation are solved self-consistently [1].

Nevertheless, the similarity conditions are unlikely attainable in real experiments because of many practical and physical constraints. In the comparison between the existing ICRF JET experiments and ITER heating scenarios, the scaling of the machine size is almost fixed as $\eta_R \approx 2$, but other scaling parameters unlikely satisfy the relations of Eq. (1) except the matched scaling of the magnetic fields and the wave frequency, $\eta_\omega = \eta_B$. In the previous study [2], we evaluated several important effects of the deviations from the similarity conditions between JET and ITER for the ICRF minority heating scenario of (³He) D-T plasmas [2,3,4,5]. In the scenario, the scaling parameters are $\eta_\omega = \eta_B = 1.44$, $\eta_R = 2.0$, $\eta_n = 2.63$, $\eta_{I_p} = 4.0$, $\eta_{n\Phi} = 1.0$, $\eta_{I_p} = 4.5$, $\eta_T = 2.0$. We found that three combinations of the above scaling parameters (D_1 , D_2 , and D_3) sufficiently describe three important ICRF phenomena (optimized minority fractions, power decompositions, and effective temperatures) by capturing damping mechanisms, kinetic effects, FLR effects, and Doppler effects, unless the deviations are significant [2].

In this proceeding, we present the analysis of the deviations from the similarity for the different scenario of (^3He) H plasmas. We evaluate the important impact of the changes in the plasma density, temperature, wave toroidal mode number between JET and ITER.

2. EXACT SCALING RELATIONS

The exact similarity relations are obtained by the scaling of the coupled equations of Maxwell's equation with the plasma current, Grad-Shafranov equation, Fokker-Planck equations. Because the plasma dielectric tensor of the Maxwell's equation is a function of several dimensionless parameters by

$$\epsilon = \epsilon \left(\frac{\omega_p}{\omega}, \frac{\omega_c}{\omega}, \frac{k_{\parallel} v_t}{\omega}, k_{\perp} \rho \right), \quad (2)$$

the same dielectric tensor requires the conditions of plasmas $\eta_{\omega}=\eta_B$, $\eta_n=\eta_B^2$ in Eq. (1). By the normalization of the Maxwell's equation, the exact scaling of the length and the time scale of the wave requires $\eta_{\omega}=\eta_R$.

The scaling of toroidal mode number ($\eta_{n\Phi}$) determines the scaling of the parallel refractive index (η_{\parallel}) by

$$\eta_{\parallel} = \eta_{n\Phi} / (\eta_R \eta_{\omega}). \quad (3)$$

When η_R , $\eta_{\omega}=1$ and $\eta_T=1$ are satisfied as in Eq. (1), the same toroidal mode results in the same perpendicular refractive index because the wave dispersion relation with the same dielectric tensor of Eq. (2) are the same. The scaling condition of the plasma current and the total power in Eq. (1) are obtained by satisfying the scaling of the Grad-Shafranov equation and the Bounce-averaged Fokker-Planck equations, respectively [1].

3. DEVIATIONS FROM THE EXACT SCALING

In this section, we investigated the effects of the scaling parameter changes in ITER compared to the existing JET experimental parameters, which do not satisfy the exact scaling conditions in Eq. (1), for the (^3He) H heating scenario. Besides the effects shown in [2], we additionally show the effect of the plasma current scaling in this study. As a reference of JET experiment, we use the parameters, $\omega=37\text{MHz}$, $R=3\text{m}$, $B_0=3.8\text{T}$, $I_p=2\text{MA}$, $n_0=0.25 \times 10^{20}\text{m}^{-3}$, $T_0=6\text{KeV}$, $n_{\Phi}=27$, $P=5\text{MW}$ of the discharge 63322 [6]. Then, for the ITER heating scenario, we use the scaling parameters, $\eta_{\omega}=\eta_B=1.5$, $\eta_R=2.0$, $\eta_n=4.0$, $\eta_p=4.0$, $\eta_{n\Phi}=1.0$, $\eta_{lp}=4.5$, $\eta_T=4.0$ for the simulations. In the following three subsections, we find the impact of the change by η_T , $\eta_{n\Phi}$, η_n , and η_{lp} .

3.1 Temperature and toroidal mode dependency

Figure 1 shows the optimized fraction of the minority density to the electron density n_{He^3}/n_e for the maximum ion damping percentage by the simulations of the full wave code, TORIC [7]. The majority ion damping and IBW electron damping are also calculated, but they are negligibly small in these simulations. Hence, the total power absorption is approximately the summation of the fundamental damping of the minority ion ^3He and the electron Landau damping of the fast wave branch. The minority fraction is scanned from $n_{\text{He}^3}/n_e=0.01$ to $n_{\text{He}^3}/n_e=0.1$, as shown in Figure 1-(a), to find the optimal ratio for the maximum ion damping (and the minimum electron damping) in Figure 1-(b).

As shown in [2], the ICRF wave damping mechanism depending on the minority fraction can be explained the scaling parameter D_1 ,

$$D_1 = \frac{\eta_{n\Phi} \sqrt{\eta_T}}{\eta_B \eta_R}, \quad (4)$$

which represents the scaling of the ratio of resonance width by Doppler effect to the effective damping length [8]. As shown in Figure 1-(a), the dependency of ion damping on the minority fraction between JET (black curve) and ITER (red curve) are very similar, if $D_1=1$ and the refractive index does not change $\eta_{n\Phi}=\eta_R \eta_{\omega}=3$. As the refractive index decreases while keeping $D_1=1$, the ion damping is reduced, but the optimal concentration for the ion maximum damping unlikely changes (see the red and green curves). As D_1 changes, the optimal fraction changes accordingly.

Figure 1-(b) shows that the optimal minority fraction is almost proportional to the scaling parameter D_1 in the range of the interest. The approximate formula for the optimal minority fraction in the (He^3) H heating scenario is $n_{\text{He}^3}/n_e \approx 0.03 D_1$, regardless of the changes in the plasma temperature and the toroidal mode number. The optimal minority concentration of the $n=1$ damping is about $n_{\text{He}^3}/n_e \approx 0.03$ for JET ($D_1=1$) and $n_{\text{He}^3}/n_e \approx 0.02$ for ITER ($D_1=0.667$). The effect of the plasma density on the optimized fraction is found to be negligibly small.

3.2 Density dependency

Figure 2 shows the similar increase of the power partition to electrons via Landau damping as the increase of the scaling parameter D_2 .

$$D_2 = \frac{\sqrt{\eta_T \eta_n}}{\eta_B}, \quad (5)$$

which represents the scaling of plasma beta [2]. The increase of the plasma density results in the increase of the wave vector of the fast wave branch and the increase of the electron damping by the multi-path damping, which is captured by the scaling of the plasma beta in D_2 . Here, the power partition is calculated in the TORIC simulations at the optimal minority concentration estimated in Figure 1-(b), which is $n_{\text{He}3}/n_e = 0.02$ for ITER. For the (^3He) H heating scenario, the scaling of ITER has $D_2=2.73$ compared to the JET experiments $D_2=1$, so we expect the increase of the electron damping from 10% to 30% approximately from Figure 2.

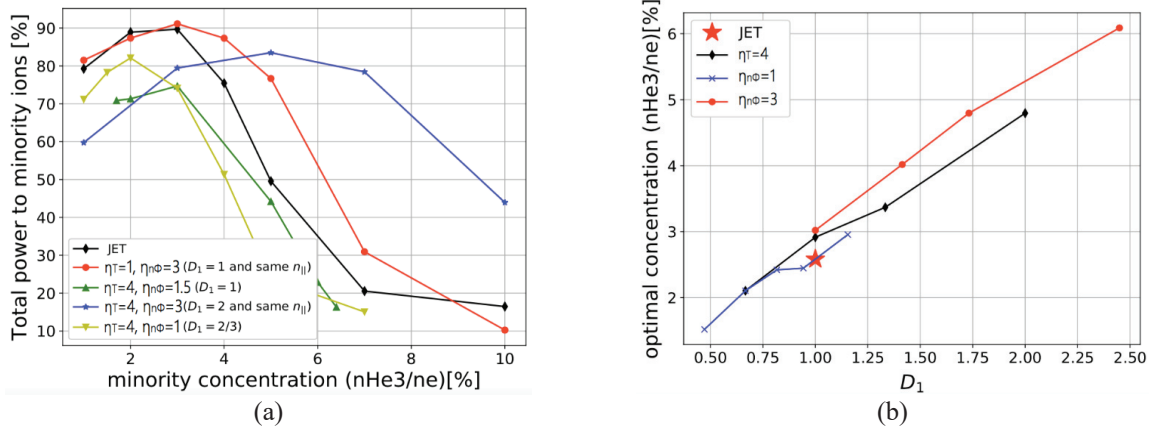


FIGURE 1. (a) Minority ion fundamental ($n=1$) damping percentage in terms of the minority fraction and (b) the optimized minority fraction for the maximum ion damping in terms of D_1 in Eq. (4) for (^3He) H plasmas. For ITER results, $\eta_\omega=\eta_B=1.5$, and $\eta_R=2$ are used. The parameters $\eta_{n\Phi}$ and η_T are adjusted for the different D_1

The contour plot in Figure 3 shows the effects of the parameter D_1 as well as D_2 on the power decomposition at the optimal minority fraction obtained in Figure 1 (i.e. $n_{\text{He}3}/n_e=0.03D_1$). The ion damping decreases as the increase of D_2 by increasing the electron damping as shown in Figure 2. Because the electron Landau damping likely occurs more when the wave interacts with thermal electrons for the larger parallel refractive index, the electron damping generally increases by D_1 , which represents the scaling of the Doppler effect. Thus, it shows somewhat decrease of the ion damping by the increase of D_1 , as shown for the part of $D_1 \leq 1.0$. However, the power decomposition is affected by D_1 significantly if the scaling changes the wave cut-off condition, which determines the evanescence wave at the edge with the small density by $\mathcal{R} - n_{\parallel}^2 < 0$. Here, $\mathcal{R} = 1 - \sum_s \omega_{ps}^2 / (\omega_{cs}(\omega + \omega_{cs}))$ is a Stix dielectric component [8], which results in the scaling of the marginal cut-off condition, $(\overline{n_{\parallel}^2} / \mathcal{R}) = (n_{\parallel}^2 / \mathcal{R})$. Here, the value with the overline is the value after the scaling. Then, for $\mathcal{R} \gg 1$, the scaling of the density for the cut-off range can be simplified by $(D_1/D_2) > (D_{1,ref}/D_{2,cut})$, where $D_{2,cut}$ corresponds to the density satisfying the evanescence condition marginally for most poloidal modes at the reference parameters for $D_{1,ref}$. For the ITER simulation parameter of $D_{1,ref}=0.667$, $D_{2,cut}$ is about 0.6, giving $D_1/D_2 > 1.1$ for the scaling of the cut-off forbidden range, as shown in the gray region in Figure 3.

4 CONCLUSIONS

In this proceeding, we explore the dependency of some plasma parameters on ICRF physics by finding the deviations of the scaling using D_1 and D_2 . The dependency of D_3 is shown in [2]. They capture the dominant mechanism of the optimal concentration, the energy partition, and the effective temperature increase, if the scaled system is not significantly different from the reference system (in other words, the change of D_1 , D_2 , and D_3 from

$D_1=1, D_2=1$ and $D_3=1$ are small). This scaling may not be universal if the global physics of ICRF changes significantly. For example, as shown in the difference Fig 1-(b) of this paper and Fig. 1-(a) of [2], the two difference species combinations of minority damping, (^3He) H plasmas and (H) D-T plasmas in [2], have the different scaling relation in terms of D_1 for the optimized minority fraction. Nevertheless, within the small deviations in the parameter space, the scaling holds effectively, as shown in the linear slopes of both figures.

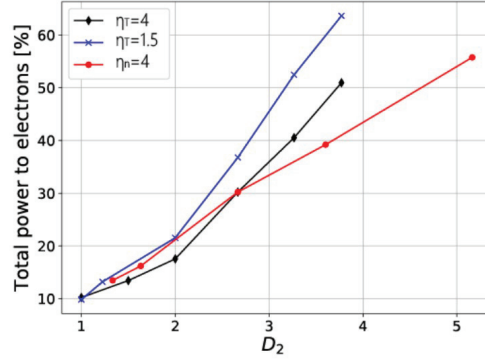


FIGURE 2. Electron damping percentage in terms of D_2 with the optimized concentration $n_{\text{He3}}/n_e = 0.02$ by fixing $D_1 = 0.667$ (black curve: $\eta_{n\Phi}=1$ for $\eta_I=4$, and blue curve: $\eta_{n\Phi}=1.616$ for $\eta_I=1.5$) for the ITER conditions of $\eta_\omega=\eta_B=1.5$, and $\eta_R=2$.

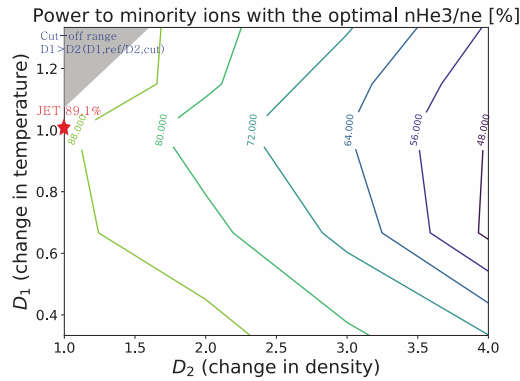


FIGURE 3. Contour plot of the ion damping percentage in terms of D_1 and D_2 at the optimal minority fraction for the ITER conditions. D_1 is adjusted by the different temperature, and D_2 is adjusted by the different density.

ACKNOWLEDGMENTS

This work was supported by the National Research Foundation of Korea (NRF) grant funded by the Korea government (MSIT) (NRF-2019R1F1A1058298)

REFERENCES

1. J. P. Lee, D. Smithe, E. F. Jaeger, P. T. Bonoli and R. W. Harvey, *Phys. Plasmas* **26**, 012505 (2019)
2. J. P. Lee, R. Bilato, E. F. Jaeger, "Analysis of the deviation from the similarity between JET and ITER ion cyclotron resonance heating", *Nucl. Fusion*, **59**, 0126006 (2019)
3. Start D. F. H. et al, *Nucl. Fusion* **39**, 321 (1999)
4. ITER Physics Expert Group on Energetic Particles, Heating and Current Drive and ITER Physics Basis Editors, *Nucl. Fusion* **39**, 2495 (1999)
5. Budny R.V., Berry L, Bilato R. et. al. *Nuclear Fusion* **52**, 023023 (2012)
6. Lamalle P.U., Mantsinen. M. J., Noterdaeme J.-M. et al., *Nuclear Fusion* **46**, 391_{SEP}(2006)
7. M. Brambilla, *Plasma Physics and Controlled Fusion* **41**, 1 (1999).
8. Porkolab M. AIP Conference Proceedings **314**, 99_{SEP}(1994)
9. Stix T. H., *Waves in Plasmas* (AIP Press) ISBN 0-88318-859-7_{SEP}(1992)